ACS Medicinal Chemistry Letters

Letter

pubs.acs.org/acsmedchemlett

Optimization of a Fragment-Based Screening Hit toward Potent DOT1L Inhibitors Interacting in an Induced Binding Pocket

Clemens Scheufler, Henrik Möbitz, Christoph Gaul, Christian Ragot, Céline Be, César Fernández, Kim S. Beyer, Ralph Tiedt, and Frédéric Stauffer*

Novartis Institutes for Biomedical Research, 4002 Basel, Switzerland

Supporting Information

ABSTRACT: Mixed lineage leukemia (MLL) gene rearrangement induces leukemic transformation by ectopic recruitment of disruptor of telomeric silencing 1-like protein (DOT1L), a lysine histone methyltransferase, leading to local hypermethylation of H3K79 and misexpression of genes (including HoxA), which drive the leukemic phenotype. A weak fragment-based screening hit identified by SPR was cocrystallized with DOT1L and optimized using structure-based ligand optimization to yield compound **8** (IC_{50} = 14 nM). This series of inhibitors is structurally not related to cofactor SAM and is not interacting within the SAM binding pocket but induces a pocket adjacent to the SAM binding site.

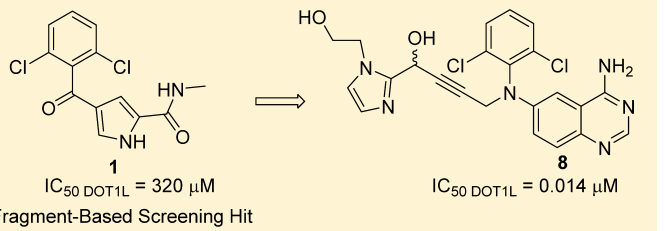

KEYWORDS: *Dot1L, lysine histone methyltransferase, inhibitor, fragment-based screen, structure-based design*

The importance of the epigenetic control of gene expression and its deregulation in cancer has been under growing focus over the recent years. Histone methyltransferases (HMTs) are a class of enzymes that introduce methyl marks on lysines and arginines of histone proteins. The lysine methyltransferases (KMTs) are responsible for mono-, di-, and trimethylation of the ε-amino group of histone lysines using the cofactor *S*-adenosyl methionine (SAM) as methyl source and are modulating directly and indirectly, via "readers", the chromatin structure, the gene expression, and the transcription regulation. An etiological role of KMTs in different types of cancers has been proposed, and pharmacological tool compounds targeting KMTs have been identified to address the relationship between alteration of histone methylation and malignant transformation.[1−3] In MLL-rearranged leukemia, DOT1L is aberrantly recruited by MLL fusion proteins and facilitates the transcription of genes critical for leukemia such as homobox (HOX) genes and myeloid ecotropic viral integration site 1 homologue (MEIS1).[4] DOT1L was described as the only known KMT responsible for methylations of lysine K79 on histone H3[5] until a recent report suggested that the SET domain containing interleukin-5 response element II binding protein (RE-IIBP) also acts as a HMT for H3K79.[6] No antagonizing demethylase for this site was identified so far. Structurally, DOT1L distinguishes itself from the other KMTs by the absence of the common SET domain and is more closely related to the arginine methyltransferase (RMT) class.[7]

Reported DOT1L inhibitors to date are mostly related to cofactor SAM and its byproduct *S*-adenosyl homocysteine (SAH)[8] with the exception of a recent report of a micromolar inhibitor discovered by virtual screening.[9] Pioneering work by researchers at Epizyme led to the discovery of the clinical candidate EPZ-5676 by modifying in several iterations the methionine moiety attached to adenosine.[10,11] Other researchers, at Baylor College and at the Structural Genomics Consortium, have disclosed similar DOT1L inhibitors with some modifications of the adenosyl moiety.[12,13] All of these inhibitors were shown to interact with DOT1L at the SAM binding pocket and display a SAM-competitive behavior. In this report, we are disclosing the discovery of new DOT1L inhibitors, which do not interact within the SAM binding pocket but induce a pocket adjacent to the SAM binding site. The superimposition of the cocrystal structures of SAM and fragment hit **1** bound to DOT1L shows no spatial overlap of the two ligands (Figure 1). However, in a biochemical assay, **1** and its analogues are SAM-competitive because, upon binding, they are engaging the lid loop of the SAM binding pocket and form a conformation incompatible with efficient SAM binding.

Fragment-based screening using surface plasmon resonance (SPR)[14] was applied to an immobilized DOT1L construct (amino acids 1−416) encompassing the N-terminal catalytic domain. We identified compound **1** as a weak binder with an estimated equilibrium binding constant of $K_D \approx 50$ μM. The biochemical activity of this hit was measured by a scintillation proximity assay (SPA), using tritium labeled cofactor SAM at concentration equal to K_M and excess of biotinylated nucleosome as substrate (Supporting Information), and resulted in a moderate inhibition (IC_{50} = 320 μM) (Table 1). Further, the compound was confirmed to bind DOT1L by

Received: April 21, 2016
Accepted: June 1, 2016

DOI: 10.1021/acsmedchemlett.6b00168
ACS Med. Chem. Lett. XXXX, XXX, XXX−XXX

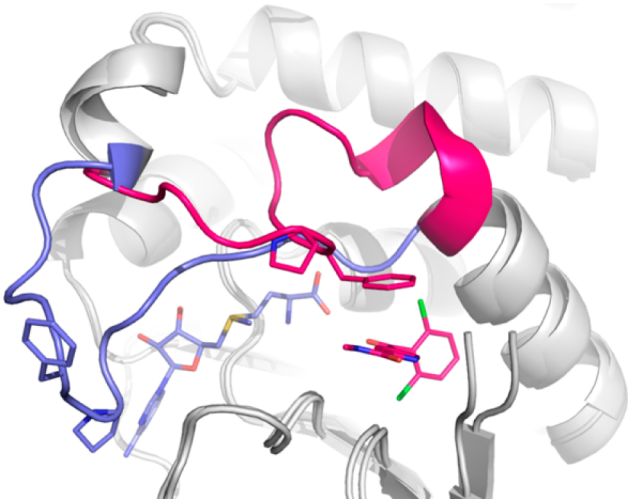

Figure 1. Superimposition of SAM bound DOT1L cocrystal structure (PDB 1nw3) and compound **1** bound DOT1L cocrystal structure (PDB 5dtm). The ligand and lid loop of the SAM binding pocket (residues 126−140, Pro130 and Phe131 shown as sticks) are colored in blue for Dot1L·SAM and magenta for Dot1L·**1**. The flexible loop 296−309 at the crystal interface is omitted for clarity. PyMol was used for structural visualization and figure preparation.[20]

NMR protein observation experiments on $^{13}C^{\varepsilon}$-methionine labeled samples[15] and subsequently was cocrystallized with DOT1L. Protein crystal structure analysis revealed the details of the binding mode (Figure 2A). The 2,6-dichlorophenyl moiety of compound **1** acts as a hydrophobic anchor occupying a hydrophobic cavity formed by side chain movements of Met147, Leu143, Phe239, and Tyr312. The 3-(2-*N*-methylaminocarbonyl)pyrrolyl moiety is sandwiched between Phe243, Pro130, and Phe131 engaging the flexible lid loop of the SAM pocket in a novel conformation by $\pi-\pi$ stacking. Such reorganization of the lid loop was also induced by the compounds described by Chen et al. in the Companion Paper.[16] Compound **1** also makes several weak, often water-mediated hydrogen bonds: the carbonyl group with Asn241, the N−H of the pyrrole with the backbone carbonyl of Ser311, and the *N*-methyl amide with Asp241 and Ser311 via two water molecules (Figure 2A).

Compound **1** was considered a suboptimal fragment hit. First, **1** is a large fragment with 19 heavy atoms and a molecular weight of 300 Da.[17] Its interactions with the protein are dominated by hydrophobic and stacking interactions. The hydrogen bond interactions with the protein are suboptimal in distance and orientation or are water-mediated. As a consequence, the ligand efficiency of **1** (LE = 0.25) is at the low end of what one would expect for a good fragment hit (Table 1).[18] In addition, compound **1** is inducing its pocket, potentially limiting the impact of structure-based ligand optimization due to the expected plasticity of the induced pharmacophore. However, with a good understanding of the limitations of our chemical starting point and extensive X-ray crystallographic support available, we initiated hit optimization by fragment growing.

The *N*-methylamide of compound **1** was modified to a 3-pyridyl in order to extend the stacking moiety and to maintain the hydrogen bond acceptor capability of the amide via the pyridyl nitrogen. In addition, a substituent was introduced at position 5 of the pyridyl to replace the water-mediated hydrogen bond of the amide NH by a direct interaction with

Table 1. Biochemical Activity of Compounds 1−10 with General Formula

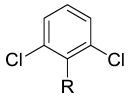

cps	R group	IC_{50}[a] [μM]	LE[b]
1	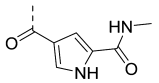	320	0.25
2	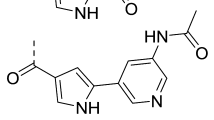	4.3	0.29
3	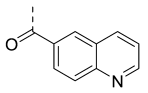	139	0.26
4	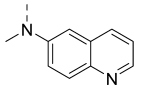	98	0.28
5	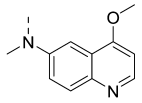	39	0.28
6	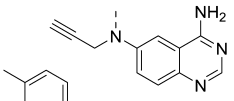	0.92	0.36
7	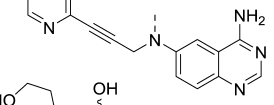	0.047	0.34
8	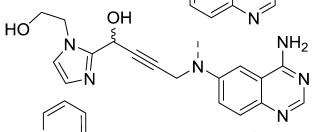	0.014	0.33
9	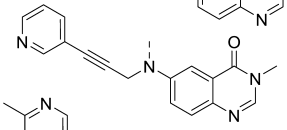	0.84	0.28
10	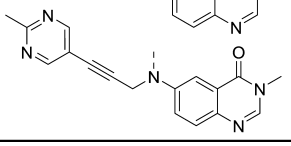	0.089	0.31

[a]SPA assay; geometric means of duplicates. [b]Ligand efficiency (LE) calculated from IC_{50} as surrogate for K_d.

Asn241. An acetylamino substituent (compound **2**, IC_{50} = 4.3 μM), where the carbonyl can approach Asn241 at H-bonding distance, was found to be optimal. Another way to extend the stacking capability of the initial hit (compound **1**) was realized by linking the 2,6-dichlorophenylcarbonyl moiety to a bicyclic heteroaryl system such as 6-quinolinyl (compound **3**, IC_{50} = 139 μM).

Analysis of the cocrystal structure of compound **3** with DOT1L (5dtq) indicates that the 2,6-dichlorophenyl is filling optimally the hydrophobic backpocket limiting the opportunity for gaining affinity in this part of the molecule. Notably, the carbonyl oxygen of compound **3** is not engaging Asn241 in a hydrogen bond interaction (Figure 2B). In order to open a new growth vector at this position, an isosteric replacement of the ketone by a methylamino group was shown to be suitable (compound **4**, IC_{50} = 98 μM). Formally, compounds **3** and **4** could be still considered fragments with a molecular weight of 300 Da, equal to our initial hit (compound **1**). The ligand

DOI: 10.1021/acsmedchemlett.6b00168
ACS Med. Chem. Lett. XXXX, XXX, XXX−XXX

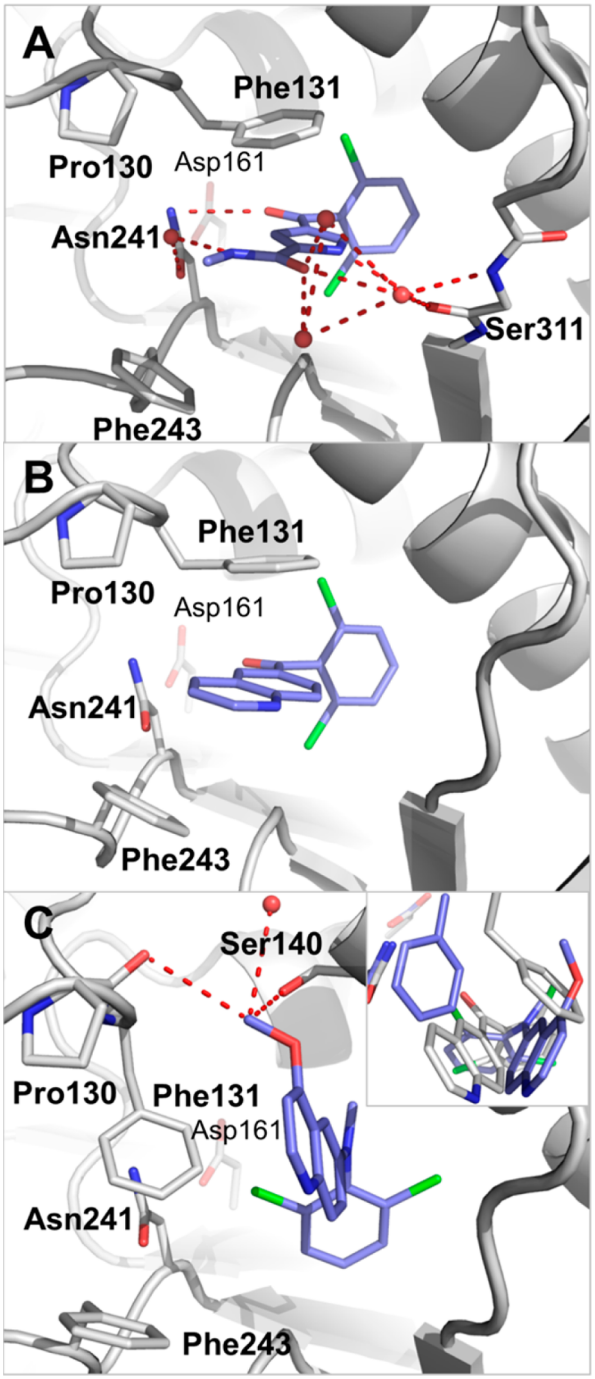

Figure 2. X-ray cocrystal structures of Dot1L (gray) with **1** (A), **3** (B), and **5** (C). Amino acids engaged in key interactions with the ligand (blue) are illustrated as sticks. (Water mediated) Hydrogen bonds with Dot1L are shown as dotted red lines. The binding mode flip from **3** (gray) to **5** (blue) is shown as insert in (C).

efficiencies of compounds **3** and **4** (LE = 0.26 and 0.28, respectively) slightly exceed that of compound **1** despite the fact that we decreased the hydrogen bond capabilities of those new ligands while improving their stacking/hydrophobic interactions. In contrast to the cocrystal structure of DOT1L with EPZ-5676 (4hra) where the lid loop is partially disordered, **1** and **3** are engaging the lid loop and interact efficiently with Phe131 (Figures 1 and S2).

Introduction of a methoxy group at position 4 of the quinoline (compound **5**, IC_{50} = 39 μM) designed to provide an acceptor for a direct hydrogen bond with Asn241 triggered an unexpected binding mode shift as shown by cocrystallization of DOT1L with compound **5** (Figure 2C, 5dtr). Although the 2,6-dichlorophenyl hydrophobic anchor is still interacting in the same pocket as observed for compounds **1** and **3**, Phe131 of the flexible SAM pocket lid loop is swinging around the quinoline bicycle and now is forming an edge-to-face interaction with the quinoline, which is flanked on the other face by Leu143 and Val310. The methoxy group is not acting as a hydrogen bond acceptor for Asn241 as originally designed but rather as a donor of three pseudo hydrogen bonds from the polarized C−H of the methyl group to a water molecule, Ser140 and Pro130 (Figure 2C).

The growth vector emerging from the amino group at position 6 of the quinoline is a quite narrow channel formed by Phe131, Ser140, Val169, Phe239, and Asn241 (Figure S1). We further optimized compound **5** by modifying the quinolinyl stacking moiety to the equipotent but more electron deficient quinazolinyl, and by introducing an amino group at position 4 of the quinazoline in order to form a hydrogen bond interaction with the hydroxyl group of Ser140. We then extended the N-Me to an N-propargyl substituent (compound **6**, IC_{50} = 0.92 μM) to optimally pass through the narrow hydrophobic channel (Figure S1). Compound **6**, containing 23 heavy atoms, is the most efficient ligand (LE = 0.36) reported herein, and the jump in efficiency compared to compound **4** is mostly driven by the introduction of the 4-amino hydrogen bond donor that is optimally interacting with Ser140.

The cocrystal structure of compound **5** indicates that the narrow hydrophobic channel opens toward a solvent accessible pocket, with Asn241 and Ser140 providing the first polar interaction opportunities. We could demonstrate that growing the terminal position of **6** with a 5-methylpyridin-2-yl was favorable, positioning a hydrogen bond acceptor for Ser140 (compound **7**, IC_{50} = 0.047 μM). Docking of compound **7** revealed that Ser140 is sandwiched between the hydrogen bond donor amino group at position 4 of the quinazoline and the pyridyl hydrogen bond acceptor (Figure 3). The cocrystal structure of a closely related inhibitor to compound **7** with DOT1L confirms a similar binding mode as for compound **5** and the predicted bidentate interaction with the Ser140

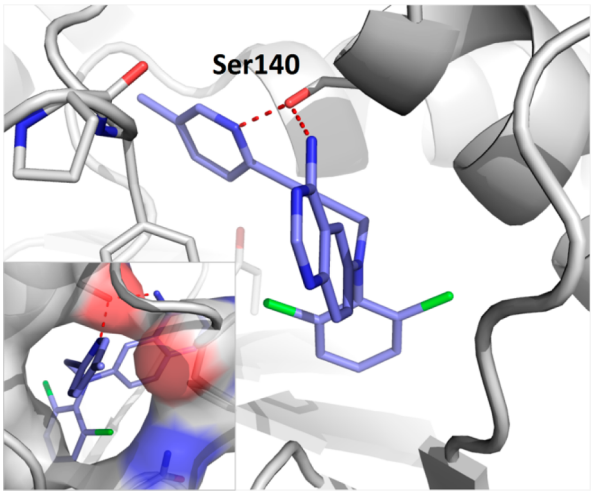

Figure 3. Docking of compound **7**, highlighting chelation of Ser140, in the cocrystal structure of DOT1L·**5**. View of the ligand going through the narrow hydrophobic channel to reach Ser140 is shown as insert.

DOI: 10.1021/acsmedchemlett.6b00168
ACS Med. Chem. Lett. XXXX, XXX, XXX−XXX

hydroxyl group (structure not shown). Finally, the most optimal group that we have identified to go through the narrow channel and interact in the pocket at the exit of the channel was the *N*-(4-hydroxy-4-(1-(2-hydroxyethyl)-1*H*-imidazol-2-yl)but-2-yn-1-yl) substituent (compound **8**, IC_{50} = 0.014 μM).

We hypothesized that the shift of binding mode observed between compounds **3** and **5** was not the result of changing the carbonyl to the N-Me group but rather the consequence of the methoxy group serving as a hydrogen bond donor for Ser140. We went back to investigate the initial binding mode using 3-methyl-4-oxo-3,4-dihydroquinazolinyl as stacking moiety with a hydrogen bond acceptor only at position 4 and extending through the narrow channel with a 3-pyridylpropargyl substituent in order to position adequately the nitrogen acceptor to interact with Ser140 hydroxyl (compound **9**, IC_{50} = 0.84 μM), similarly to what was achieved with compound **7**. Further optimization was accomplished with the introduction of a second symmetrical nitrogen and a methyl at position 2 of the pyrimidine (compound **10**, IC_{50} = 0.089 μM). The cocrystal structure of compound **10** with DOT1L is a confirmation of the predicted binding mode comparable to **3**. The quinazolinone stacking moiety of **10** is sandwiched between Phe243 and Phe131 and is engaged in a hydrogen bond interaction with Asn241 (structure not shown).

Compound **2** was obtained by Friedel–Crafts acylation with 2,6-dichlorobenzoyl chloride of the corresponding heteroaryl intermediate. Compound **3** was obtained by manganese dioxide oxidation of the alcohol resulting from the attack on 2,6-dichlorobenzaldehyde with the Grignard originating from 6-bromoquinoline (Scheme 1). Syntheses of compounds **4**–**10** involve an initial Buchwald–Hartwig coupling of 2,6-dichloroaniline on the suitable bromo-bicyclic heteroaryl partner followed by alkylation of the aniline nitrogen. Extension of the terminal position of the propargyl group was achieved by Sonogashira coupling with the suitable halogenoheteroaryl or by deprotonation and nucleophilic attack on a known aldehyde. For some of the derivatives, further functional group manipulations were applied as shown in Scheme 2.

Scheme 1. Synthesis of Compounds 2 and 3[a]

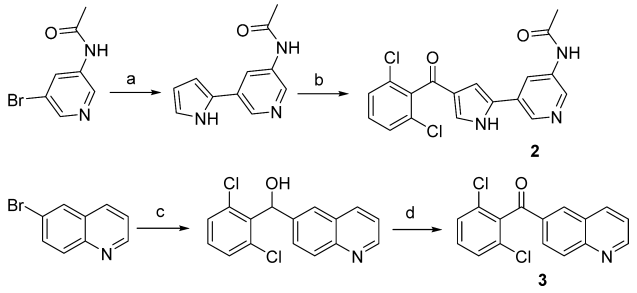

[a]Reagents and conditions: (a) (i) 1-Boc-pyrrole-2-boronic acid pinacol ester, $Pd(dbpf)Cl_2$, Cs_2CO_3, THF/water, 50 °C, 13 h; (ii) TFA, rt, 1 h, yield 98%; (b) 2,6-dichlorobenzoyl chloride, $AlCl_3$, CH_2Cl_2, rt, 25.5 h, yield 8%; (c) (i) methylmorpholine, *n*-BuLi, THF/hexane, −78 °C, 1 h; (ii) $MgBr_2{\cdot}Et_2O$, −78 °C, 90 min; (iii) 2,6-dichlorobenzaldehyde, THF, −78 °C, 3.5 h, yield 24%; (d) MnO_2, $CHCl_3$, rt, 94 h, yield 36%.

In conclusion, we discovered a new class of DOT1L inhibitors by optimizing a weak fragment-based screening hit displaying suboptimal interactions in an induced binding pocket. By fine-tuning the stacking interactions, replacing water mediated hydrogen bond interactions by direct hydrogen bonds, and opening a new vector for fragment growing, we were able to increase affinity by more than 4 orders of magnitude. We have witnessed a binding mode shift triggered by very subtle modifications of the ligand. Both binding modes were exploited, based on our structural understanding, for further specific optimization. Finally, we demonstrated for the first time the possibility to potently inhibit DOT1L catalytic activity without interacting in the SAM binding site.

Scheme 2. Synthesis of Compounds 4–10[a]

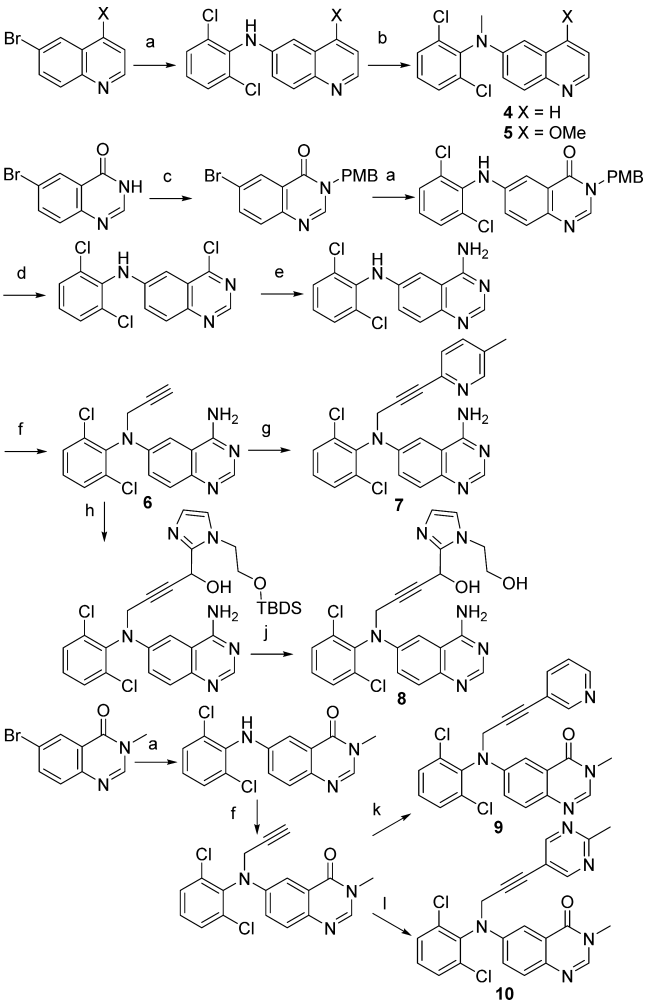

[a]Reagents and conditions: (a) 2,6-dichloroaniline, Cs_2CO_3, Xantphos, $Pd_2(dba)_3{\cdot}CHCl_3$, dioxane, 100 °C, 17–19 h, yields 69–81%; (b) (i) 55% NaH in oil, DMF, rt, 30 min; (ii) CH_3I, rt, 2–15 h, yields 73–75%; (c) (i) 55% NaH in oil, DMF, rt, 30 min; (ii) 4-methoxybenzyl chloride, rt, 145 min, yield 95%; (d) (i) TFA/water, 90 °C, 48 h, yield 88%; (ii) $POCl_3$, DMF, 100 °C, 3 h, yield 99%; (e) NH_3, dioxane, 170 °C, 16 h, yield 97%; (f) (i) 55–60% NaH in oil, DMF, rt, 20–30 min; (ii) propargyl bromide, rt, 105–120 min, yields 64–92%; (g) 2-bromo-5-methylpyridine, CuI, $Pd(PPh_3)_2Cl_2$, NEt_3, NMP, rt, 17 h, yield 63%; (h) (i) EtMgBr, THF, rt, 1 h; (ii) 1-(2-((*tert*-butyldimethylsilyl)oxy)-1*H*-imidazole-2-carbaldehyde,[19] rt, 20 min, yield 65%; (j) HF·pyridine, THF, rt, 1.5 h, yield 22%; (k) 3-iodopyridine, CuI, $Pd(PhCN)_2Cl_2$, $^tBu_3PHBF_4$, iPr_2NH, dioxane, rt, 17.75 h, yield 20%; (l) 5-bromo-2-methylpyrimidine, CuI, $Pd(PPh_3)_2Cl_2$, NEt_3, NMP, rt, 19.5 h, yield 22%.

DOI: 10.1021/acsmedchemlett.6b00168
ACS Med. Chem. Lett. XXXX, XXX, XXX–XXX

■ ASSOCIATED CONTENT

Supporting Information

The Supporting Information is available free of charge on the ACS Publications website at DOI: 10.1021/acsmedchemlett.6b00168.

Figures S1 and S2, synthetic procedures, compound characterizations, and assay protocols (PDF)

■ AUTHOR INFORMATION

Corresponding Author

*E-mail: frederic.stauffer@novartis.com.

Author Contributions

The manuscript was written through contributions of all authors. All authors have given approval to the final version of the manuscript.

Notes

The authors declare the following competing financial interest(s): Authors are shareholders of Novartis and/or employees of Novartis.

■ ACKNOWLEDGMENTS

The authors thank Aurelie Winterhalter, Julia Klopp, Patrick Graff, Elke Koch, Paul James Westwood, Christophe Mura, and Aurore Roustan for excellent technical assistance.

■ REFERENCES

(1) DeCarlo, D.; Hadden, M. K. Oncoepigenomics: Making histone lysine methylation count. *Eur. J. Med. Chem.* **2012**, *56*, 179−194.

(2) Kaniskan, H. Ü.; Jin, J. Chemical Probes of Histone Lysine Methyltransferases. *ACS Chem. Biol.* **2015**, *10*, 40−50.

(3) McGrath, J.; Trojer, P. Targeting histone lysine methylation in cancer. *Pharmacol. Ther.* **2015**, *150*, 1−22.

(4) Okada, Y.; Feng, Q.; Lin, Y.; Jiang, Q.; Li, Y.; Coffield, V. M.; Su, L.; Xu, G.; Zhang, Y. hDOT1L links histone methylation to leukemogenesis. *Cell* **2005**, *121*, 167−178.

(5) Nguyen, A. T.; Zhang, Y. The Diverse Functions of Dot1 and H3K79 Methylation. *Genes Dev.* **2011**, *25*, 1345−1358.

(6) Woo Park, J.; Kim, K.-B.; Kim, J.-Y.; Chae, Y.-C.; Jeong, O.-S.; Seo, S.-B. RE-IIBP Methylates H3K79 and Induces MEIS1-mediated Apoptosis via H2BK120 Ubiquitination by RNF20. *Sci. Rep.* **2015**, *5*, 12485.

(7) Min, J.; Feng, Q.; Li, Z.; Zhang, Y.; Xu, R.-M. Structure of the Catalytic Domain of Human Dot1L, a Non-SET Domain Nucleosomal Histone Methyltransferase. *Cell* **2003**, *112*, 711−723.

(8) Anglin, J. L.; Song, Y. A Medicinal Chemistry Perspective for Targeting Histone H3 Lysine-79 Methyltransferase DOT1L. *J. Med. Chem.* **2013**, *56*, 8972−8983.

(9) Chen, S.; Li, L.; Chen, Y.; Hu, J.; Liu, J.; Liu, Y.-C.; Liu, R.; Zhang, Y.; Meng, F.; Zhu, K.; Lu, J.; Zheng, M.; Chen, K.; Zhang, J.; Yao, Z.; Luo, C. Identification of Novel Disruptor of Telomeric Silencing 1-like (DOT1L) Inhibitors through Structure-Based Virtual Screening and Biological Assays. *J. Chem. Inf. Model.* **2016**, *56*, 527−534.

(10) Anglin, J. L.; Deng, L.; Yao, Y.; Cai, G.; Liu, Z.; Jiang, H.; Cheng, G.; Chen, P.; Dong, S.; Song, Y. Synthesis and Structure Activity Relationship Investigation of Adenosine-containing Inhibitors of Histone Methyltransferase DOT1L. *J. Med. Chem.* **2012**, *55*, 8066−8074.

(11) Daigle, S. R.; Olhava, E. J.; Therkelsen, C. A.; Basavapathruni, A.; Jin, L.; Boriack-Sjodin, P. A.; Allain, C. J.; Klaus, C. R.; Raimondi, A.; Scott, M. P.; Waters, N. J.; Chesworth, R.; Moyer, M. P.; Copeland, R. A.; Richon, V. M.; Pollock, R. M. Potent Inhibition of Dot1L as Treatment of MLL-Fusion Leukemia. *Blood* **2013**, *122*, 1017−1025.

(12) Yu, W.; Smil, D.; Li, F.; Tempel, W.; Fedorov, O.; Nguyen, K. T.; Bolshan, Y.; Al-Awar, R.; Knapp, S.; Arrowsmith, C. H.; Vedadi, M.; Brown, P. J.; Schapira, M. Bromo-deaza-SAH: A potent and selective DOT1L inhibitor. *Bioorg. Med. Chem.* **2013**, *21*, 1787−1794.

(13) Deng, L.; Zhang, L.; Yao, Y.; Wang, C.; Redell, M. S.; Dong, S.; Song, Y. Synthesis, activity and metabolic stability of non-ribose containing inhibitors of histone methyltransferase DOT1L. *MedChemComm* **2013**, *4*, 822−826.

(14) Retra, K.; Irth, H.; van Muijlwijk-Koezen, J. E. Surface Plasmon Resonance biosensor analysis as a useful tool in FBDD. *Drug Discovery Today: Technol.* **2010**, *7*, e181−e187.

(15) Gelis, I.; Bonvin, A. M. J. J.; Keramisanou, D.; Koukaki, M.; Gouridis, G.; Karamanou, S.; Economou, A.; Kalodimos, C. G. Structural Basis for Signal-Sequence Recognition by the Translocase Motor SecA as Determined by NMR. *Cell* **2007**, *131*, 756−769.

(16) Chen, C.; Zhu, H.; Stauffer, F.; Caravatti, G.; Vollmer, S.; Machauer, R.; Holzer, P.; Möbitz, H.; Scheufler, C.; Klumpp, M.; Tiedt, R.; Beyer, K. S.; Calkins, K.; Guthy, D.; Kiffe, M.; Zhang, J.; Gaul, C. Discovery of Novel Dot1L Inhibitors through a Structure-Based Fragmentation Approach. *ACS Med. Chem. Lett.* **2016**, 10.1021/acsmedchemlett.6b00167. Companion paper.

(17) Jhoti, H.; Williams, G.; Rees, D. C.; Murray, C. W. The 'rule of three' for fragment-based drug discovery: where are we now? *Nat. Rev. Drug Discovery* **2013**, *12*, 5−7.

(18) Bembenek, S. D.; Tounge, B. A.; Reynolds, C. H. Ligand efficiency and fragment-based drug discovery. *Drug Discovery Today* **2009**, *14*, 278−283.

(19) Berdini, V.; Saxty, G.; Angibaud, P. R.; Querolle, O. A. G.; Poncelet, V. S.; Roux, B.; Meerpoel, L. Anticancer pyridopyrazines via the inhibition of FGFR kinases. WO2013/061080 A1, May 2, 2013.

(20) *The PyMOL Molecular Graphics System*, version 1.5.0.4; Schrödinger, LLC.

DOI: 10.1021/acsmedchemlett.6b00168
ACS Med. Chem. Lett. XXXX, XXX, XXX−XXX